Royal Netherlands
Meteorological Institute
Ministry of Infrastructure
and Water Management

Epicenters for the Lauwerzijl and Kommerzijl events on 17-11-2022

E. Ruigrok, P. Kruiver

De Bilt, 2022 | Technical report; TR-402

Royal Netherlands
Meteorological Institute
Ministry of Infrastructure
and Water Management

Epicenters for the Lauwerzijl and Kommerzijl events on 17-11-2022

KNMI, R&D Seismology and Acoustics

December 9, 2022

Introduction

On 17-11-2022 two events occurred within one hour. The first event is the Lauwerzijl event at 11:27:43.79 UTC with a local magnitude of 1.7 , the second event is the Kommerzijl event at 12:18:37 UTC with a local magnitude of 1.1. Both events were detected by the KNMI network (*KNMI*, 1993) and located near-real time with the Hypocenter method (*Lienert et al.*, 1986). These fast solutions use an average 1D model for the north of the Netherlands (*Kraaijpoel and Dost*, 2013).

In this report, the epicenters are improved by using a best-fitting traveltime versus distance model based on a database of local P-wave traveltime picks. This data-driven model incorporates actual underburden velocities and only well pickable phase arrivals. An error estimate is derived from the spread in picking times from the best-fitting model. This error incorporates both the local variations of the velocity field as well as picking errors. These errors are propagated further into an epicentral probability density function (PDF). This results into updated epicenters and their 95% confidence regions.

On 7-4-2018 there was a similar sequence of events at the Kommerzijl gas field. A M1.7 in Lauwerzijl (07:17:49.39 UTC) was followed by a M1.0 in Kommerzijl (08:25:05.79 UTC).

Lauwerzijl

Fig. 1 shows the seismic sensors where manual P-wave picks are available for the Lauwerzijl event. A grid search is performed for a region around the Hypocenter solution, as indicated by the red box in Fig. 1. In the first step, equal differential time (EDT, *Zhou*, 1994) residuals are computed. That is, for each grid point and for each station combination, the traveltime differences are forward modelled and tabulated. From these values, the observed traveltime differences are subtracted to obtain the EDT residuals. In the second step, the PDF is derived from the EDT residuals, using a L1 norm (*Tarantola*, 2005). Fig. 2 shows the 95% confidence area of the resulting PDF. The location with the maximum probability is assigned to be the updated epicenter.

The following list contains the new epicenter both in wgs84 coordinates and in the Dutch national triangulation system (RD). The line that surrounds the 95% confidence zone is by approximation an ellipse. The parameters of this ellipse (major axis, minor axis and orientation) are listed, together with a gridded version of this contour.

Epicenter in wgs84 [deg]: 6.3073, 53.3088

Epicenter in RD [m]: 216330, 591760

Ellipse major axis [m]: 933

Ellipse minor axis [m]: 558

Orientation of the major axis [deg]: 160.9

95% confidence contour RDx [m]: 216373, 216420, 216478, 216510, 216540, 216570, 216600, 216616, 216630, 216635, 216640, 216637, 216630, 216623, 216607, 216596, 216571, 216558, 216540, 216510, 216480, 216452, 216421, 216390, 216360, 216330, 216270, 216210, 216152, 216120, 216090, 216070, 216057, 216039, 216031, 216030, 216034, 216043, 216060, 216068, 216090, 216104, 216120, 216150, 216177, 216200, 216228, 216261, 216300, 216330, 216373

95% confidence contour RDy [m]: 591310, 591301, 591310, 591323, 591344, 591376, 591425, 591460, 591520, 591550, 591610, 591670, 591714, 591760, 591820, 591850, 591910, 591940, 591971, 592019, 592059, 592090, 592120, 592146, 592166, 592180, 592200, 592201, 592180, 592157, 592123, 592090, 592060, 592000, 591940, 591880, 591820, 591760, 591700, 591670, 591614, 591580, 591550, 591499, 591460, 591430, 591400, 591370, 591342, 591324, 591310

The waveform data used in the above analysis is publicly available and can be obtained through:

GUI: http://rdsa.knmi.nl/dataportal/

FDSN webservices: http://rdsa.knmi.nl/fdsnws/dataselect/1/

PGV values

The following table contains peak ground velocity (PGV) values as obtained at nearby accelerometers. The 'max rotated' PGV is listed, which is the maximum particle velocity in the horizontal plane. For the computation of the 'max rotated' PGV, a time window around the S-wave arrival is used and the maximum value of the resultant of both horizontal components is taken.

Station name	Epicentral distance [km]	PGV [mm/s]
GK020	1.30	0.337
GK030	2.91	0.241
GK010	4.48	0.178
G740	5.48	0.152
G760	7.21	0.055
GK040	7.07	0.106
KMP	7.77	0.079
G730	9.14	0.053
G750	11.98	0.093
G780	13.61	0.076
G720	13.38	0.109
G160	15.25	0.046
SRHV	16.16	0.037
G210	19.04	0.041
OSTM	19.99	0.020

Table 1: Recorded PGVs for the Lauwerzijl 17-11-2022 event.

Kommerzijl

Fig. 3 shows the seismic sensors where manual P-wave picks are available for the Kommerzijl event. A grid search is done for a region around the Hypocenter solution, as indicated by the red box in Fig. 3. Fig. 4 shows the 95% confidence area of the resulting PDF. The location with the maximum probability is assigned to be the updated epicenter.

The following list contains the new epicenter both in wgs84 coordinates and in the Dutch national triangulation system (RD). The line that surrounds the 95% confidence zone is by approximation an ellipse. The parameters of this ellipse (major axis, minor axis and orientation) are listed, together with a gridded version of this contour.

This event has a magnitude too small to list PGV values. Only for events with magnitude larger than 1.5, there is a chance that the 2 mm/s threshold is reached (*Ruigrok and Dost*, 2020).

Epicenter in wgs84 [deg]: 6.3018, 53.3058

Epicenter in RD [m]: 215970, 591420

Ellipse major axis [m]: 2099

Ellipse minor axis [m]: 919

Orientation of the major axis [deg]: 145.9

95% confidence contour RDx [m]: 216114, 216210, 216300, 216360, 216421, 216476, 216507, 216523, 216525, 216510, 216488, 216459, 216421, 216390, 216344, 216300, 216243, 216197, 216146, 216090, 216029, 215962, 215886, 215820, 215752, 215670, 215580, 215490, 215400, 215307, 215220, 215160, 215125, 215119, 215134, 215160, 215195, 215239, 215280, 215329, 215370, 215430, 215481, 215526, 215580, 215633, 215672, 215725, 215760, 215814, 215856, 215910, 215977, 216114

95% confidence contour RDy [m]: 590580, 590577, 590603, 590640, 590700, 590790, 590880, 590970, 591090, 591204, 591300, 591390, 591480, 591545, 591630, 591699, 591780, 591840, 591900, 591960, 592020, 592080, 592140, 592188, 592230, 592275, 592314, 592341, 592355, 592350, 592316, 592256, 592170, 592050, 591960, 591870, 591780, 591690, 591618, 591540, 591480, 591398, 591330, 591270, 591197, 591120, 591060, 590970, 590910, 590820, 590760, 590697, 590640, 590580

Conclusion

Both events have an epicenter that maps on top of the western part of the Kommerzijl gas field. Also their 95% confidence zones map largely within the field. The Lauwerzijl M1.7 event is located in the northeastern corner of the field. The Kommerzijl M1.1 event is situated more towards the middle of the gas field, at 0.50 km from the previous event. A location at the Grijpskerk gas storage can be excluded.

The highest recorded PGV of 0.337 mm/s is at station GK020 at 1.3 km from the Lauwerzijl M1.7 event.

References

KNMI (1993), Netherlands Seismic and Acoustic Network, Royal Netherlands Meteorological Institute (KNMI), Other/Seismic Network, doi:10.21944/e970fd34-23b9-3411-b366-e4f72877d2c5.

Kraaijpoel, D., and B. Dost (2013), Implications of salt-related propagation and mode conversion effects on the analysis of induced seismicity, *Journal of Seismology*, *17*(1), 95–107.

Lienert, B. R., E. Berg, and L. N. Frazer (1986), HYPOCENTER: An earthquake location method using centered, scaled, and adaptively damped least squares, *Bulletin of the Seismological Society of America*, *76*(3), 771–783.

Ruigrok, E., and B. Dost (2020), Advice on the computation of peak-ground-velocity confidence regions for events in gas fields other than the Groningen gas field, *KNMI Technical Report*, *TR-386*.

Tarantola, A. (2005), *Inverse Problem Theory and Methods for Model Parameter Estimation*, SIAM, Philadelphia.

Zhou, H.-w. (1994), Rapid three-dimensional hypocentral determination using a master station method, *Journal of Geophysical Research: Solid Earth*, *99*(B8), 15,439–15,455.

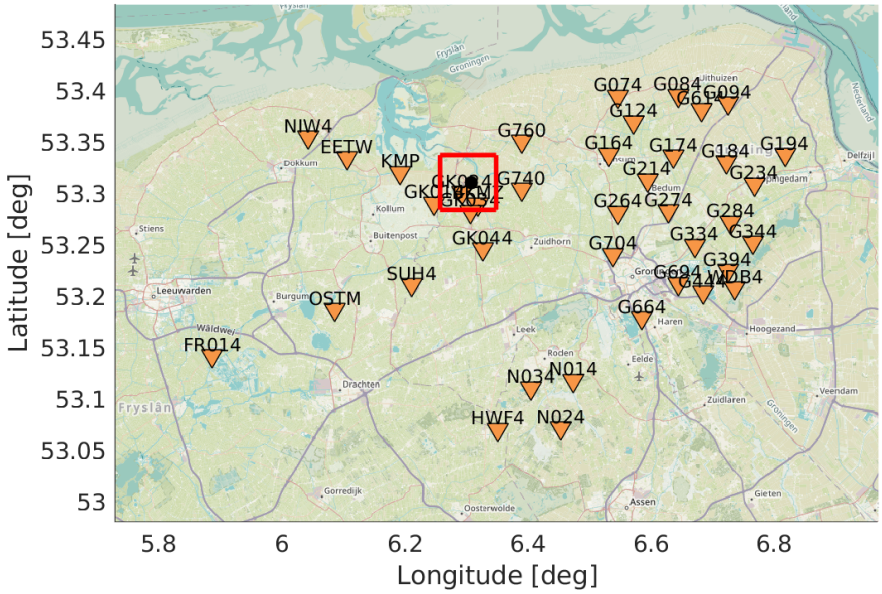

Figure 1: Overview map for the Lauwerzijl event with locations of stations (orange triangles) where P-wave onsets were picked, the fast Hypocenter solution (black dot) and the boundary line of the area in which a grid search is done (red box). Background map is from www.openstreetmap.org.

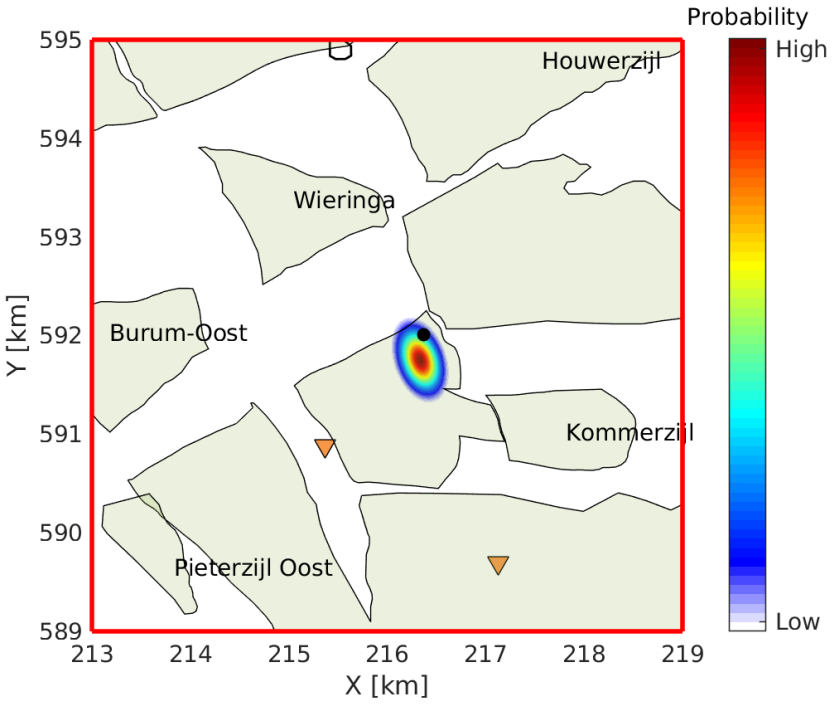

Figure 2: Map showing hydrocarbon fields (green-filled polygons), the fast Hypocenter solution (black dot) and the epicentral probability density function (PDF) of the Lauwerzijl event using time-differences and an optimized model. The coloured area is the 95% confidence zone of the PDF. The field polygons are from www.nlog.nl, using the March 2020 update.

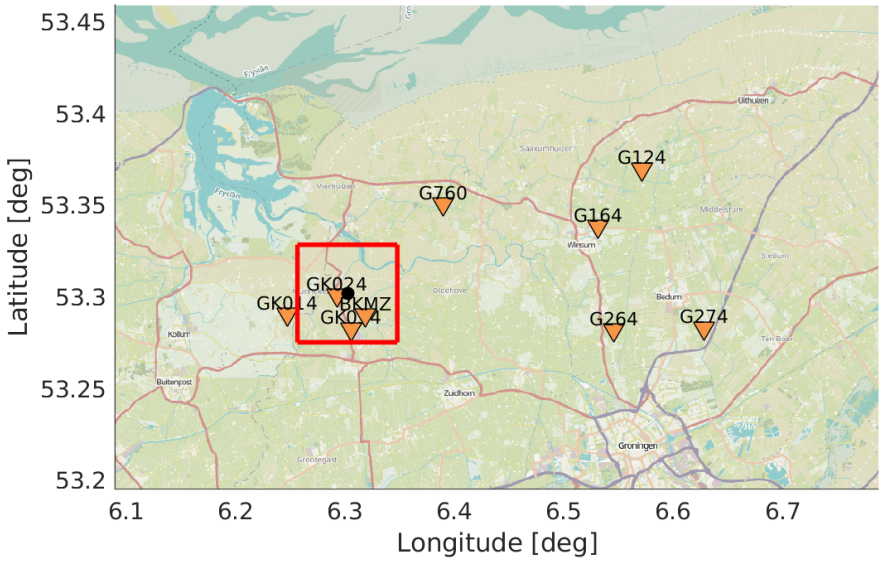

Figure 3: Overview map for the Kommerzijl event with locations of stations (orange triangles) where P-wave onsets were picked, the fast Hypocenter solution (black dot) and the boundary line of the area in which a grid search is done (red box). Background map is from www.openstreetmap.org.

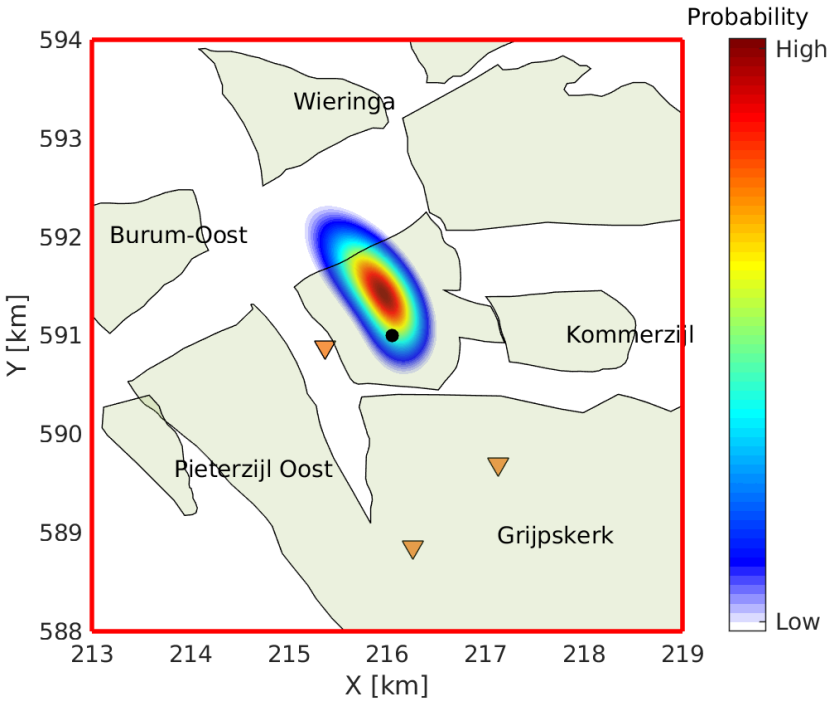

Figure 4: Map showing hydrocarbon fields (green-filled polygons), the fast Hypocenter solution (black dot) and the epicentral probability density function (PDF) of the Kommerzijl event using time-differences and an optimized model. The coloured area is the 95% confidence zone of the PDF. The field polygons are from www.nlog.nl, using the March 2020 update.

Royal Netherlands Meteorological Institute

PO Box 201 | NL-3730 AE De Bilt
Netherlands | www.knmi.nl